

## Magnetic Moments of Chromium-Doped Gold Clusters: The Anderson Impurity Model in Finite Systems

K. Hirsch,<sup>1,2,\*</sup> V. Zamudio-Bayer,<sup>1,2</sup> A. Langenberg,<sup>1,2</sup> M. Niemeyer,<sup>1,2</sup> B. Langbehn,<sup>1,2</sup> T. Möller,<sup>1</sup>  
A. Terasaki,<sup>3,4</sup> B. v. Issendorff,<sup>5</sup> and J. T. Lau<sup>2,†</sup>

<sup>1</sup>*Institut für Optik und Atomare Physik, Technische Universität Berlin, Hardenbergstraße 36, 10623 Berlin, Germany*

<sup>2</sup>*Institut für Methoden und Instrumentierung der Forschung mit Synchrotronstrahlung,*

*Helmholtz-Zentrum Berlin für Materialien und Energie GmbH, Albert-Einstein-Straße 15, 12489 Berlin, Germany*

<sup>3</sup>*Cluster Research Laboratory, Toyota Technological Institute, 717-86 Futamata, Ichikawa, Chiba 272-0001, Japan*

<sup>4</sup>*Department of Chemistry, Kyushu University, 6-10-1 Hakozaki, Higashi-ku, Fukuoka 812-8581, Japan*

<sup>5</sup>*Physikalisches Institut, Universität Freiburg, Stefan-Meier-Straße 21, 79104 Freiburg, Germany*

(Received 26 April 2013; revised manuscript received 10 November 2014; published 25 February 2015)

The magnetic moment of a single impurity atom in a finite free electron gas is studied in a combined x-ray magnetic circular dichroism spectroscopy, charge transfer multiplet calculation, and density functional theory study of size-selected free chromium-doped gold clusters. The observed size dependence of the local magnetic moment can be understood as a transition from a local moment to a mixed valence regime. This shows that the Anderson impurity model essentially describes finite systems even though the discrete density of states introduces a significant deviation from a bulk metal, and the free electron gas is only formed by less than 10 electrons. Electronic shell closure in the gold host minimizes the interaction of localized impurity states with the confined free electron gas and preserves the magnetic moment of  $5\mu_B$  fully in  $\text{CrAu}_2^+$  and almost fully in  $\text{CrAu}_6^+$ . Even for open-shell species, large local moments are observed that scale with the energy gap of the gold cluster. This indicates that an energy gap in the free electron gas stabilizes the local magnetic moment of the impurity atom.

DOI: 10.1103/PhysRevLett.114.087202

PACS numbers: 75.75.-c, 36.40.Cg, 75.20.Hr, 78.20.Ls

The interaction of localized impurity states with a free electron gas [1] leads to such complex phenomena as Friedel oscillations [2] or the Kondo effect [3]. The properties of magnetic impurities in nonmagnetic bulk metals [4] have therefore been subject of intense research over the last 50 years. Considerable advances in the understanding of these many-body effects have been achieved by photoemission, x-ray magnetic circular dichroism (XMCD), and scanning tunneling spectroscopy of adatoms [5–10], clusters on surfaces [11], or well-defined quantum dots [12,13]. This allows the study of fundamental parameters such as the on site Coulomb repulsion or the amount of interaction of the impurity atom with the host metal. In all these cases, however, the impurity atom is in contact with a bulk free electron gas that has a continuous density of states at the Fermi energy. In contrast, the study of single impurities in size-selected clusters would allow us to characterize the interaction of localized electronic states with a finite free electron gas, i.e., with a well-defined number of electrons and a highly discrete density of states, for which the bulk concept of metals does not apply [14,15]. Because this introduces a new parameter for the control of electronic and magnetic properties, isolated transition-metal-doped coinage-metal clusters have been studied intensively by density functional theory (DFT) calculations [16,17] and experiment: their electronic and geometrical structure as well as their relative stability have been probed by photoelectron [18–20],

infrared photodissociation [21,22], and ultraviolet photo-fragmentation [23,24] spectroscopy, as well as by electron diffraction [25]. Yet, none of these experimental techniques directly addresses magnetic properties. Here, we study chromium-doped gold clusters as model systems that combine considerable local magnetic moments, carried by the  $3d$  electrons of the impurity atom, with a finite free electron gas formed by the gold host. We investigate the magnetic moment of a single chromium impurity by local and element-specific XMCD spectroscopy of size-selected gas phase clusters [26–30]. The results of our combined experimental and theoretical study show that the size dependence of the local magnetic moment in the finite, isolated system  $\text{CrAu}_n^+$  is correlated with the variation of the energy gap at the Fermi energy of the host cluster. This can essentially be understood within the Anderson impurity model [1] despite the significant modification that is introduced by the energy gap and by the discrete density of states in a finite system.

Experimentally, x-ray absorption and XMCD spectra were recorded in ion yield mode with a combined linear ion trap and superconducting solenoid setup [27–35] that has sufficient sensitivity to study singly doped size-selected free clusters [28,36,37]. The cluster beam is produced in a magnetron gas aggregation source by cosputtering of chromium and gold targets, mass selected in a quadrupole mass filter, and transferred into the radio frequency ion trap by electrostatic and radio frequency ion guides. Inside the ion

trap, the doped gold clusters are magnetized by an external 5 T magnetic field under continuous helium buffer gas cooling to an ion temperature of  $(12 \pm 4)$  K. Resonant photoexcitation at the  $L_{2,3}$  absorption edges of chromium was performed at BESSY II beamline UE52-PGM. After x-ray absorption, the core-excited cluster ions relax via cascading Auger decay, which leads to photofragmentation of the parent ion [32,33,38]. The photoion yield was recorded at the chromium  $L_{2,3}$  edges for linear as well as for circular polarization with parallel and antiparallel alignment of photon helicity and magnetic field. The resulting x-ray absorption spectra in Fig. 1 were normalized to the incident photon flux and scaled to unity at the  $L_3$  edge. The XMCD signal was normalized to photon flux and number of unoccupied  $3d$  states as inferred from the integrated x-ray absorption signal to directly reflect the amount of magnetization. These experimental spectra allow us to obtain local and element specific information on the electronic and magnetic structure of the chromium impurity in  $\text{CrAu}_n^+$  clusters. This holds true even though the XMCD spin sum rule [39] cannot be applied to chromium because of

intermixing  $2p_{3/2} \rightarrow 3d$  and  $2p_{1/2} \rightarrow 3d$  transitions [40,41] even for seemingly well separated lines. Nevertheless, quantitative information on the electronic structure and the local magnetic moment can be obtained from comparison to charge transfer multiplet calculations [42,43], shown in Fig. 1. This is possible for  $\text{CrAu}_n^+$ ,  $n = 2, 5-7$ , where we were able to model the experimental spectra. The resulting weights of the electronic configurations that contribute to the ground state are given in Fig. 1. To further analyze the electronic and magnetic properties of  $\text{CrAu}_n^+$ , established ground state geometries [16] were reoptimized in a Kohn-Sham DFT framework as implemented in the QUANTUM ESPRESSO 5.0 plane wave code [44], employing the Perdew-Burke-Ernzerhof approximation to the exchange-correlation functional [45]. For more information see Supplemental Material [46] and references therein [47-49].

As can be seen from the nonvanishing XMCD signals in Fig. 1, all  $\text{CrAu}_n^+$  clusters under study exhibit local and total magnetic moments that are oriented in the presence of the external magnetic field independent of the detailed geometric

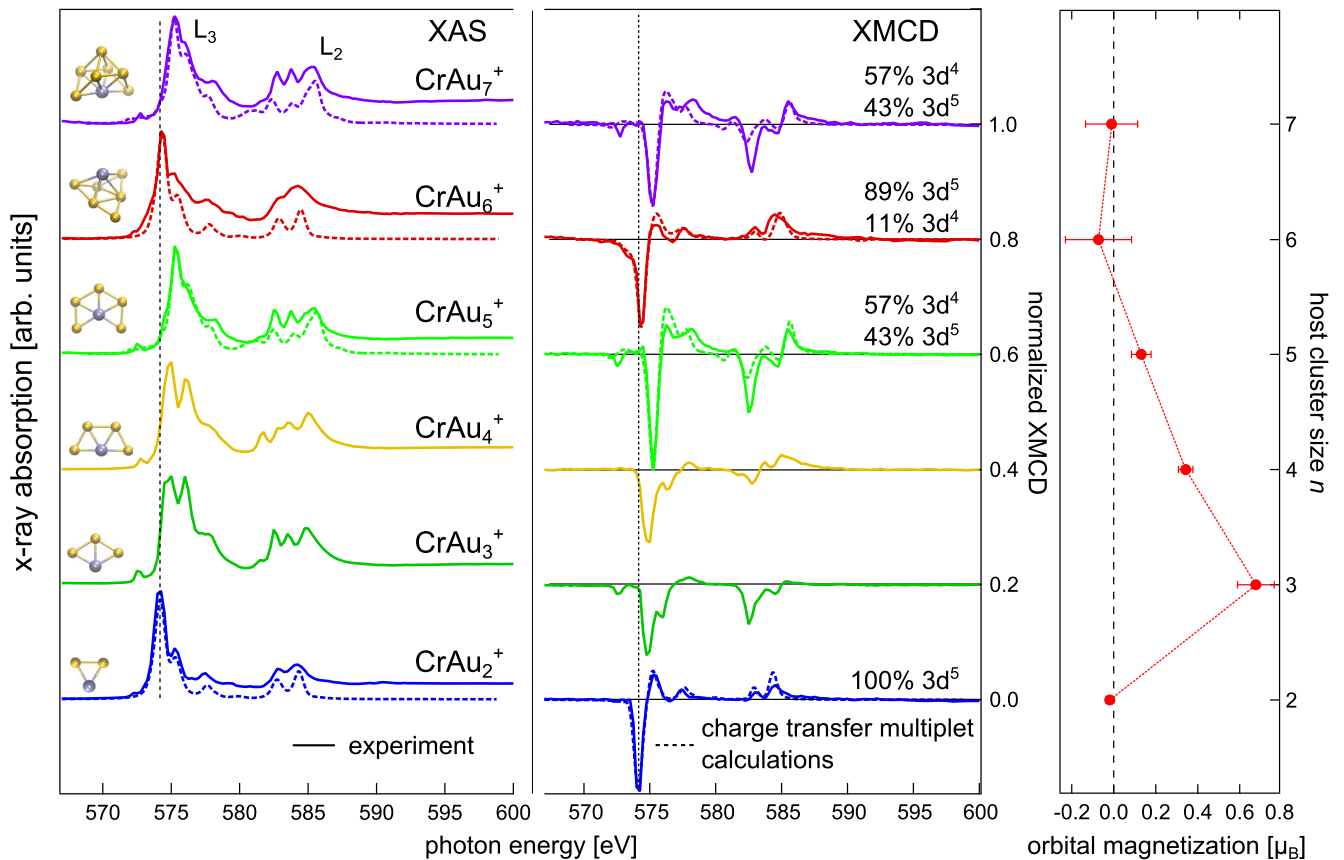


FIG. 1 (color online). Left: Linear x-ray absorption spectra (solid lines) of  $\text{CrAu}_n^+$  clusters,  $n = 2-7$ , normalized to the  $L_3$  maximum intensity and overlaid with theoretical spectra (dashed lines) of  $\text{CrAu}_n^+$ ,  $n = 2, 5-7$ , from charge transfer multiplet calculations next to relaxed ground state structures [16] (dark atom: chromium; light atoms: gold). Center: Corresponding XMCD spectra (solid lines) of  $\text{CrAu}_n^+$ , normalized to the number of unoccupied  $3d$  states and theoretical spectra (dashed lines) from charge transfer multiplet calculations, giving the weight of configurations that contribute to the ground state. Right: Measured orbital magnetization at the experimental conditions of  $T = (12 \pm 4)$  K and  $\mu_0 H = 5$  T.

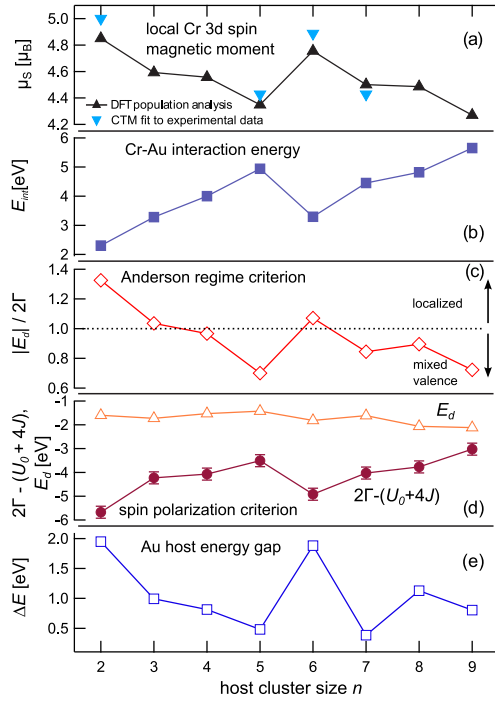


FIG. 2 (color online). (a) Calculated local chromium spin magnetic moments  $\mu_S$  of  $\text{CrAu}_n^+$  from a DFT population analysis (black upwards triangles) and from charge transfer multiplet (CTM) calculations fitted to the experimental data (blue downwards triangles); (b) Cr-Au interaction energy  $E_{\text{int}}$ ; (c) Anderson regime criterion  $|E_d|/2\Gamma$ ; (d) criterion for full spin polarization  $E_d > 2\Gamma - (U_0 + 4J)$ , using  $J = 0.75 \pm 0.25$  eV; (e) energy gap  $\Delta E$  of the  $\text{Au}_n$  host in the geometry of  $\text{CrAu}_n^+$ .

and electronic structure. The spin magnetic moments of  $\text{CrAu}_n^+$ ,  $n = 2, 5-7$ , extracted from the charge transfer multiplet calculations are shown in Fig. 2(a). These values are in excellent agreement with local chromium spin magnetic moments obtained from DFT calculations by projecting the Kohn-Sham orbitals onto atomic wave functions.

The spin magnetic moment of almost  $5\mu_B$  in  $\text{CrAu}_n^+$ ,  $n = 2, 6$ , originates from a nearly pure  $3d^5$  configuration of the chromium impurity. This strong atomic localization of the  $3d$  electrons at the chromium site is also reflected in screening effects that shift the maximum of the  $L_3$  absorption line and XMCD asymmetry in Fig. 1 by  $\approx 0.5$  eV to lower excitation energy [32,50] for  $\text{CrAu}_n^+$ ,  $n = 2, 6$  as compared to  $n = 3-5, 7$ . For  $\text{CrAu}_2^+$ , a fit of the calculated XMCD asymmetry to the experimental spectrum yields an alignment of  $0.48 \pm 0.05$ , which corresponds to the Brillouin value for a total spin  $S = 5/2$  at  $B = 5$  T and  $T = (14 \pm 3)$  K. This agrees well with the experimental conditions of  $T = (12 \pm 4)$  K. Thus, the magnitude of the XMCD asymmetry further confirms a spin magnetic moment of  $5\mu_B$  in  $\text{CrAu}_2^+$ .

In case of  $\text{CrAu}_n^+$ ,  $n = 2, 6$ , we expect the magnetization to be solely due to the spin contribution, since a half filled  $3d$  shell does not carry orbital angular momentum. This can

indeed be shown experimentally because the XMCD orbital sum rule is very robust and can be applied to the early transition metal chromium [41]. The orbital magnetization extracted from the XMCD data is shown in the right panel of Fig. 1. As expected, the orbital moments in  $\text{CrAu}_n^+$  are zero within the error bars for  $n = 2, 6$  whereas significant orbital contributions can be found for  $n = 3, 4$ . These finite orbital momenta imply that the ground state should be dominated by a  $3d^4$  or  $3d^6$  configuration, which reduces the spin magnetic moment as compared to the isolated chromium atom. The admixture of  $3d^4$  or  $3d^6$  configurations, manifest in the strong configuration mixing in the ground state in Fig. 1, suggests that the chromium  $3d$  electrons hybridize with gold  $5d/6s$  states not only in  $\text{CrAu}_n^+$ ,  $n = 5, 7$  but also for  $n = 3, 4$ . From the electronic ground state of  $\text{CrAu}_n^+$ ,  $n = 5, 7$ , one would expect considerable orbital momenta as well. However, these seem to be strongly reduced or quenched because of symmetry breaking where the orbital angular momentum ceases to be a good quantum number [27]. Where there is a finite orbital magnetic moment ( $n = 3-5$ ), this is aligned parallel to the spin magnetic moment as can be seen from the sign of the orbital magnetization and from the energy dependent integrals of the XMCD signals presented in the Supplemental Material [46]. The combination of XMCD spectroscopy, charge transfer multiplet, and DFT calculations shows that hybridization of the impurity  $3d$  and the host  $5d/6s$  electronic states in  $\text{CrAu}_n^+$ ,  $n = 3-5, 7$ , only leads to a reduction but not to a complete quenching of the local spin moment.

The particular behavior of  $\text{CrAu}_2^+$  and  $\text{CrAu}_6^+$  can be understood from the electronic stability of the gold host. The gold subunits of both clusters, depicted in Fig. 1, are structurally close to pure  $\text{Au}_2$  and  $\text{Au}_6$  [51]; i.e., they remain nearly undistorted when adding the chromium impurity. In  $\text{CrAu}_n^+$ ,  $n = 3-5, 7$ , in contrast, the gold host is strained and deformed in comparison to its isolated, relaxed counterpart. This enhanced stability of  $\text{Au}_2$  and  $\text{Au}_6$  stems from shell closure for two and six delocalized  $6s$  electrons [51], which, in spite of a strong  $spd$  hybridization [52], form a free electron gas confined in a two dimensional potential well [53]. Therefore,  $\text{Au}_2$  and  $\text{Au}_6$  are known to feature large second differences in binding energy and wide energy gaps  $\Delta E \approx 2$  eV at the Fermi energy [51]. Since the presence of an energy gap strongly affects the density of electronic states and thus, the amount of hybridization, a relation between  $\Delta E$  and the impurity magnetic moment can be anticipated, cf. Figs. 2(a) and 2(e). Because of the wide energy gap, the chromium cation is expected to interact more weakly in  $\text{CrAu}_n^+$ ,  $n = 2, 6$  than with the open-shell gold clusters. This is indeed true, as can be inferred from the chromium-gold interaction energy  $E_{\text{int}} = E(\text{Cr}^+) + E(\text{Au}_n) - E(\text{CrAu}_n^+)$ , shown in Fig. 2(b). To extract the contribution of the chromium interaction with the gold cluster from the total energy,  $E(\text{Au}_n)$  is

calculated in the same geometric configuration of  $\text{Au}_n$  as in  $\text{CrAu}_n^+$ . As expected, the weakest impurity-host interactions of 2.5 eV and 3.3 eV are indeed found for  $\text{CrAu}_2^+$  and  $\text{CrAu}_6^+$ , respectively. In  $\text{CrAu}_n^+$ ,  $n = 3-5, 7$ ,  $E_{\text{int}}$  increases to 3.3–5 eV and indicates an increasing amount of covalent or metallic bonding. In contrast to electronic shell closure, the coordination of the impurity atom only plays a minor role for the spin, but strongly modifies the orbital angular momentum. The spin magnetic moment of two-dimensional clusters with  $n = 2-5$  decreases only slightly even though the coordination number increases linearly and is equal to the number of gold atoms while the average chromium-gold distances remain at  $\approx 2.7 \text{ \AA}$  [46]. A similar effect is observed for larger ( $n = 6-9$ ) three-dimensional  $\text{CrAu}_n^+$  clusters. However, Fig. 2(b) also reveals that  $E_{\text{int}}$  cannot fully explain the size dependence of the magnetic moment, because this simple criterion would predict nearly identical magnetic moments and localized  $3d$  electrons for  $\text{CrAu}_6^+$  and  $\text{CrAu}_3^+$ , which is not the case as can be seen from Fig. 2.

The interaction between a magnetic impurity and the free electron host states is a crucial ingredient for the local magnetic moment in the Anderson impurity model [1]. Within this model, the magnetic moment of the impurity atom sensitively depends on the interplay of the on site Coulomb repulsion, i.e., the direct Coulomb interaction of two electrons in the same localized orbital, on the energetic position  $E_d$ , and on the width  $2\Gamma$  of the localized state. This width is determined by the coupling strength to the free electron states and by their density in the vicinity of the energy of the impurity state [1]. In the absence of any interaction with the free electron gas, the impurity states  $E_d$  and  $E_d + U_0$  are separated by the bare Coulomb interaction  $U_0$  that preserves the local magnetic moment if  $U_0$  pushes the state  $E_d + U_0$  above the Fermi level. In the presence of an interaction, virtual states are formed at energies  $E_d + U_0 \cdot n_-$  and  $E_d + U_0 \cdot n_+$ , where  $n_{\pm}$  are the occupation numbers of the impurity atom majority and minority states. The separation of the virtual levels is reduced to an effective value  $U_{\text{eff}} = U_0(n_+ - n_-)$  by hybridization of the localized impurity states with free electron gas states, which causes a broadening of the virtual states [1]. Here,  $(n_+ - n_-)$  is the spin polarization of the localized state. A generalization of the Anderson impurity model to a fivefold degenerate impurity state, as for  $3d$  elements, shows that the separation of majority and minority states is increased by the intra-atomic  $d-d$  exchange  $J$  to  $U_0 + 4J$  [54].

For a quantitative analysis of the relevant parameters  $U_0$ ,  $2\Gamma$ , and  $E_d$ , we performed DFT calculations; for details see Supplemental Material [46] and references therein [55–57]. The Anderson impurity model predicts full spin polarization of a system if  $E_d \geq 2\Gamma - (U_0 + 4J)$ , i.e., if the broadened minority spin state lies completely above the Fermi energy [58]. This criterion is fulfilled for all clusters investigated

as can be seen from Fig. 2(d). Hence, the magnetic moments of  $\text{CrAu}_n^+$  clusters have to be proportional to the  $3d$  occupation of the impurity, which is indeed the case as inferred from the charge transfer multiplet calculations.

Within the Anderson impurity model, the number of  $3d$  electrons should deviate from five for chromium if the width  $2\Gamma$  of the localized state becomes comparable to its binding energy  $E_d$ , which leads to only partial occupation of the localized state. The criterion  $|E_d|/2\Gamma$  is shown in Fig. 2(c). For  $\text{CrAu}_n^+$ ,  $n = 5, 7-9$ , we find  $|E_d|/2\Gamma < 1$ , i.e., a mixed valence state. Consequently, we have to mix the two configurations  $[\text{Ar}]3d^4$  and  $[\text{Ar}]3d^5$ , which is equivalent to a partial occupation of the  $3d$  state, in order to model the experimental XMCD spectra within the charge transfer multiplet framework. Even though  $|E_d|/2\Gamma \approx 1$ , i.e., only on the brink of a mixed valence state, we conclude that  $\text{CrAu}_n^+$ ,  $n = 3, 4$ , is indeed in a mixed valence state from the finite orbital magnetization that reveals a clear deviation from a pure  $[\text{Ar}]3d^5$  configuration. With  $|E_d|/2\Gamma \gg 1$ ,  $\text{CrAu}_2^+$  is clearly in a localized moment state, while  $\text{CrAu}_6^+$  is primarily in a localized moment state, as indicated by  $|E_d|/2\Gamma \geq 1$  and substantiated by the fact that only a small admixture of a  $3d^4$  configuration is needed to reproduce the experimental spectrum in Fig. 1. Hence, the magnetic moments observed in  $\text{CrAu}_n^+$  clusters can essentially be explained in terms of the Anderson impurity model, even though the requirement of a continuous density of states is not fulfilled.

We would like to emphasize that by varying the size of  $\text{CrAu}_n^+$  clusters different regimes of the Anderson impurity model can be prepared and probed. These are mainly determined by the size dependence of the width  $2\Gamma$  of the localized state. In particular, the local moment regime, yielding the largest magnetic moments, can be found for  $\text{CrAu}_2^+$  and  $\text{CrAu}_6^+$ , where  $2\Gamma$  is strongly reduced because of the large energy gap in the electronic density of states of the gold host. On the other hand, the energy gap  $\Delta E$  of the open shell host is reduced in  $\text{CrAu}_n^+$ ,  $n = 3-5, 7$  in comparison to  $n = 2, 6$ . This results in larger widths  $2\Gamma$  of the impurity state, and consequently, in a mixed valence state.

Finally, Fig. 2 shows that the variation of the impurity magnetic moment is only of the order of 10% for  $\text{CrAu}_n^+$  even though the energy gap  $\Delta E$  and the interaction  $E_{\text{int}}$  vary by a factor of 2. This is because even in bulk gold, i.e., in the absence of any energy gap, the chromium impurity is magnetic [59] and carries a spin magnetic moment of  $3.61 \mu_B$  [60]. The effect of reduced hybridization on this already large magnetic moment is a sizable increase of the spin magnetic moment by  $\approx 0.8-1.2 \mu_B$ . An even larger effect of the energy gap or a discrete density of states on the local magnetic moment should be observed in systems with small or even vanishing magnetic moment of the impurity in the bulk limit. In the latter case, the energy gap might even serve to restore the local magnetic moment of the impurity atom.

In summary, the experimentally observed size dependence of the magnetic moments of size-selected chromium-doped gold clusters is in line with the Anderson impurity model. The size-dependent variation of the spin magnetic moment is linked to the amount of hybridization of the impurity with the host density of states, which, in turn, is governed by the energy gap of the gold host cluster. Electronic shell closure in the gold host leads to wide energy gaps  $\Delta E$  in the free electron states. These energy gaps reduce the interaction with the impurity, increase the on site Coulomb repulsion, and lead to the maximum spin magnetic moments of almost  $5 \mu_B$  for  $\text{CrAu}_n^+$ ,  $n = 2, 6$ . This effect is a result of quantum confinement in the free electron gas and is thus unique to finite systems. It allows us to control the impurity magnetic moment by tuning the interaction with the free electron gas via quantum size effects.

Beam time for this project was granted at BESSY II beamline UE52-PGM, operated by Helmholtz-Zentrum Berlin. Technical assistance and user support by P. Hoffmann and E. Suljoti is gratefully acknowledged. Calculations were carried out on the DFG FOR 1282 computing cluster. The superconducting solenoid was provided by the Special Cluster Research Project of Genesis Research Institute, Inc. We thank L. Leppert for fruitful discussions. B. v. I. acknowledges travel support by Helmholtz-Zentrum Berlin für Materialien und Energie.

\*konstantin.hirsch@helmholtz-berlin.de

†tobias.lau@helmholtz-berlin.de

- [1] P. W. Anderson, *Phys. Rev.* **124**, 41 (1961).
- [2] J. Friedel, *Nuovo Cimento* **7**, 287 (1958).
- [3] J. Kondo, *Prog. Theor. Phys.* **32**, 37 (1964).
- [4] W. J. de Haas, J. de Boer, and G. J. van den Berg, *Physica (Utrecht)* **1**, 1115 (1934).
- [5] V. Madhavan, W. Chen, T. Jamneala, M. F. Crommie, and N. S. Wingreen, *Science* **280**, 567 (1998).
- [6] J. Li, W.-D. Schneider, R. Berndt, and B. Delley, *Phys. Rev. Lett.* **80**, 2893 (1998).
- [7] P. Gambardella, S. S. Dhesi, S. Gardonio, C. Grazioli, P. Ohresser, and C. Carbone, *Phys. Rev. Lett.* **88**, 047202 (2002).
- [8] A. J. Heinrich, J. A. Gupta, C. P. Lutz, and D. M. Eigler, *Science* **306**, 466 (2004).
- [9] P. Wahl, L. Diekhöner, M. A. Schneider, L. Vitali, G. Wittich, and K. Kern, *Phys. Rev. Lett.* **93**, 176603 (2004).
- [10] C. Carbone, M. Veronese, P. Moras, S. Gardonio, C. Grazioli, P. H. Zhou, O. Rader, A. Varykhalov, C. Krull, T. Balashov, A. Mugarza, P. Gambardella, S. Lebègue, O. Eriksson, M. I. Katsnelson, and A. I. Lichtenstein, *Phys. Rev. Lett.* **104**, 117601 (2010).
- [11] N. Néel, J. Kröger, R. Berndt, T. O. Wehling, A. I. Lichtenstein, and M. I. Katsnelson, *Phys. Rev. Lett.* **101**, 266803 (2008).
- [12] S. M. Cronenwett, T. H. Oosterkamp, and L. P. Kouwenhoven, *Science* **281**, 540 (1998).
- [13] D. Goldhaber-Gordon, H. Shtrikman, D. Mahalu, D. Abusch-Magder, U. Meirav, and M. A. Kastner, *Nature (London)* **391**, 156 (1998).
- [14] B. von Issendorff and O. Cheshnovsky, *Annu. Rev. Phys. Chem.* **56**, 549 (2005).
- [15] J. Bowlan, A. Liang, and W. A. de Heer, *Phys. Rev. Lett.* **106**, 043401 (2011).
- [16] M. B. Torres, E. M. Fernández, and L. C. Balbás, *Phys. Rev. B* **71**, 155412 (2005).
- [17] D. W. Yuan, Y. Wang, and Z. Zeng, *J. Chem. Phys.* **122**, 114310 (2005).
- [18] K. Koyasu, M. Mitsui, A. Nakajima, and K. Kaya, *Chem. Phys. Lett.* **358**, 224 (2002).
- [19] X. Li, B. Kiran, L.-F. Cui, and L.-S. Wang, *Phys. Rev. Lett.* **95**, 253401 (2005).
- [20] K. Tono, A. Terasaki, T. Ohta, and T. Kondow, *Chem. Phys. Lett.* **449**, 276 (2007).
- [21] L. Lin, P. Claes, T. Hölzl, E. Janssens, T. Wende, R. Bergmann, G. Santambrogio, G. Meijer, K. R. Asmis, M. T. Nguyen, and P. Lievens, *Phys. Chem. Chem. Phys.* **12**, 13907 (2010).
- [22] L. Lin, P. Claes, P. Gruene, G. Meijer, A. Fielicke, M. T. Nguyen, and P. Lievens, *ChemPhysChem* **11**, 1932 (2010).
- [23] S. Neukermans, E. Janssens, H. Tanaka, R. E. Silverans, and P. Lievens, *Phys. Rev. Lett.* **90**, 033401 (2003).
- [24] E. Janssens, S. Neukermans, H. M. T. Nguyen, M. T. Nguyen, and P. Lievens, *Phys. Rev. Lett.* **94**, 113401 (2005).
- [25] L.-M. Wang, J. Bai, A. Lechtken, W. Huang, D. Schooss, M. M. Kappes, X. C. Zeng, and L.-S. Wang, *Phys. Rev. B* **79**, 033413 (2009).
- [26] S. Peredkov, M. Neeb, W. Eberhardt, J. Meyer, M. Tombers, H. Kampschulte, and G. Niedner-Schatteburg, *Phys. Rev. Lett.* **107**, 233401 (2011).
- [27] M. Niemeyer, K. Hirsch, V. Zamudio-Bayer, A. Langenberg, M. Vogel, M. Kossick, C. Ebrecht, K. Egashira, A. Terasaki, T. Möller, B. v. Issendorff, and J. T. Lau, *Phys. Rev. Lett.* **108**, 057201 (2012).
- [28] V. Zamudio-Bayer, L. Leppert, K. Hirsch, A. Langenberg, J. Rittmann, M. Kossick, M. Vogel, R. Richter, A. Terasaki, T. Möller, B. v. Issendorff, S. Kümmel, and J. T. Lau, *Phys. Rev. B* **88**, 115425 (2013).
- [29] A. Langenberg, K. Hirsch, A. Ławicki, V. Zamudio-Bayer, M. Niemeyer, P. Chmiela, B. Langbehn, A. Terasaki, B. v. Issendorff, and J. T. Lau, *Phys. Rev. B* **90**, 184420 (2014).
- [30] V. Zamudio-Bayer, K. Hirsch, A. Langenberg, M. Niemeyer, M. Vogel, A. Ławicki, A. Terasaki, J. T. Lau, and B. von Issendorff, *Angew. Chem. Int. Ed.* **54** (2015).
- [31] A. Terasaki, T. Majima, and T. Kondow, *J. Chem. Phys.* **127**, 231101 (2007).
- [32] J. T. Lau, J. Rittmann, V. Zamudio-Bayer, M. Vogel, K. Hirsch, P. Klar, F. Lofink, T. Möller, and B. v. Issendorff, *Phys. Rev. Lett.* **101**, 153401 (2008).
- [33] K. Hirsch, J. T. Lau, P. Klar, A. Langenberg, J. Probst, J. Rittmann, M. Vogel, V. Zamudio-Bayer, T. Möller, and B. von Issendorff, *J. Phys. B* **42**, 154029 (2009).
- [34] K. Hirsch, V. Zamudio-Bayer, F. Ameseder, A. Langenberg, J. Rittmann, M. Vogel, T. Möller, B. v. Issendorff, and J. T. Lau, *Phys. Rev. A* **85**, 062501 (2012).
- [35] J. T. Lau, K. Hirsch, A. Langenberg, J. Probst, R. Richter, J. Rittmann, M. Vogel, V. Zamudio-Bayer, T. Möller, and B. von Issendorff, *Phys. Rev. B* **79**, 241102 (2009).

- [36] J. T. Lau, K. Hirsch, P. Klar, A. Langenberg, F. Lofink, R. Richter, J. Rittmann, M. Vogel, V. Zamudio-Bayer, T. Möller, and B. v. Issendorff, *Phys. Rev. A* **79**, 053201 (2009).
- [37] J. T. Lau, M. Vogel, A. Langenberg, K. Hirsch, J. Rittmann, V. Zamudio-Bayer, T. Möller, and B. von Issendorff, *J. Chem. Phys.* **134**, 041102 (2011).
- [38] M. Vogel, C. Kasigkeit, K. Hirsch, A. Langenberg, J. Rittmann, V. Zamudio-Bayer, A. Kulesza, R. Mitrić, T. Möller, B. v. Issendorff, and J. T. Lau, *Phys. Rev. B* **85**, 195454 (2012).
- [39] P. Carra, B. T. Thole, M. Altarelli, and X. Wang, *Phys. Rev. Lett.* **70**, 694 (1993).
- [40] G. Prümper, S. Kröger, R. Müller, M. Martins, J. Viefhaus, P. Zimmermann, and U. Becker, *Phys. Rev. A* **68**, 032710 (2003).
- [41] C. Piamonteze, P. Miedema, and F. M. F. de Groot, *Phys. Rev. B* **80**, 184410 (2009).
- [42] E. Stavitski and F. M. F. de Groot, *Micron* **41**, 687 (2010).
- [43] R. D. Cowan, *The Theory of Atomic Structure and Spectra* (University of California Press, Berkeley, 1981).
- [44] P. Giannozzi *et al.*, *J. Phys. Condens. Matter* **21**, 395502 (2009).
- [45] J. P. Perdew, K. Burke, and M. Ernzerhof, *Phys. Rev. Lett.* **77**, 3865 (1996).
- [46] See Supplemental Material at <http://link.aps.org/supplemental/10.1103/PhysRevLett.114.087202> for the XMCD integrals; the chromium coordination number; the average chromium-gold nearest neighbor distance; the relaxed and unrelaxed interaction energy; the density of states of  $\text{CrAu}_n^+$ ,  $n = 2 - 7$ ; the on-site Coulomb repulsion  $U_0$  and width  $2\Gamma$ ; and details of the charge transfer multiplet calculations.
- [47] D. Vanderbilt, *Phys. Rev. B* **41**, 7892 (1990).
- [48] P. Błoński and J. Hafner, *Phys. Rev. B* **79**, 224418 (2009).
- [49] W. Ju and Z. Yang, *Phys. Lett. A* **376**, 1300 (2012).
- [50] K. Hirsch, V. Zamudio-Bayer, J. Rittmann, A. Langenberg, M. Vogel, T. Möller, B. v. Issendorff, and J. T. Lau, *Phys. Rev. B* **86**, 165402 (2012).
- [51] H. Häkkinen and U. Landman, *Phys. Rev. B* **62**, R2287 (2000).
- [52] H. Häkkinen, *Chem. Soc. Rev.* **37**, 1847 (2008).
- [53] E. Janssens, H. Tanaka, S. Neukermans, R. E. Silverans, and P. Lievens, *New J. Phys.* **5**, 46 (2003).
- [54] K. Yosida, A. Okiji, and S. Chikazumi, *Prog. Theor. Phys.* **33**, 559 (1965).
- [55] M. Cococcioni and S. de Gironcoli, *Phys. Rev. B* **71**, 035105 (2005).
- [56] H. J. Kulik and N. Marzari, *J. Chem. Phys.* **133**, 114103 (2010).
- [57] E. Şaşıoğlu, C. Friedrich, and S. Blügel, *Phys. Rev. B* **83**, 121101(R) (2011).
- [58] A. C. Hewson, in *The Kondo Problem to Heavy Fermions (Cambridge Studies in Magnetism)*, edited by D. Edwards and D. Melville (Cambridge University Press, Cambridge, 1993).
- [59] W. D. Brewer, A. Scherz, C. Sorg, H. Wende, K. Baberschke, P. Bencok, and S. Frota-Pessôa, *Phys. Rev. Lett.* **93**, 077205 (2004).
- [60] S. Frota-Pessôa, *Phys. Rev. B* **69**, 104401 (2004).